Journal of Magnetism and Magnetic Materials 481 (2019) 122–128

Contents lists available at ScienceDirect

Journal of Magnetism and Magnetic Materials

journal homepage: www.elsevier.com/locate/jmmm

Research articles

Cetuximab and Doxorubicin loaded dextran-coated Fe_3O_4 magnetic nanoparticles as novel targeted nanocarriers for non-small cell lung cancer

Qinlu Zhang[a], Qian Liu[b], Menghan Du[b], Alphons Vermorken[b], Yali Cui[b], Lixia Zhang[c], Lili Guo[b], Le Ma[b,*], Mingwei Chen[a,*]

[a] First Affiliated Hospital of Xi'an Jiaotong University, Xi'an 710061, PR China
[b] National Engineering Research Center for Miniaturized Detection Systems, Northwest University, Xi'an 710069, PR China
[c] Department of Clinical Laboratory, Shaanxi Provincial People's Hospital, Xi'an 710069, PR China

ARTICLE INFO

Keywords:
Nanoparticles
Drug targeting
Non-small cell lung cancer
Cetuximab
Doxorubicin
Epidermal growth factor receptor

ABSTRACT

Non-small cell lung cancer (NSCLC) accounts for 80–85% of all lung cancer which is the leading cause of cancer death worldwide. Eighty percent of NSCLC patients exhibit high levels of epidermal growth factor receptor (EGFR) expression. In recent years, Doxorubicin (Dox, a widely used chemotherapeutic drug) and/or Cetuximab (Cet, an EGFR-targeted inhibitor) combined with nanoparticles for cancer therapy have attracted significant attention due to their efficient targeting and the resulting increased cytotoxicity on tumor cells. Herein, we report the effects of Dox and Cet, co-conjugated to dextran-coated Fe_3O_4 magnetic nanoparticles (Dox-NPs-Cet) on the NSCLC cell line A549, which expresses a high level of EGFR. Cytotoxicity, cell proliferation and intercellular uptake were investigated after treatment with this conjugate. The results indicate that Dox-NPs-Cet significantly suppress cell proliferation of A549 cells as compared with A549 cells treated with NPs only conjugated with Dox. In summary, our study demonstrates that Dox-NPs-Cet could serve as a promising candidate for targeted therapy of NSCLC.

1. Introduction

Lung cancer is the most common cause of cancer-related death worldwide [1–3]. Two broad classes are distinguished: non-small-cell lung carcinoma (NSCLC) and small-cell lung carcinoma. The three main subtypes of NSCLC are adenocarcinoma, squamous-cell carcinoma and large-cell carcinoma. NSCLC is the most common form of lung cancer and nearly 85–90% of lung cancer patients are diagnosed as having NSCLC [4]. Depending on the stage of the tumor, the clinical treatment strategy for NSCLC patients may include surgery, radiation therapy and chemotherapy. Regrettably the majority of patients present with already locally advanced or metastatic disease which limits the use of surgery to a minority of patients [5]. Chemotherapy is neither specific, nor selective and results in only a modest increase in survival while it involves significant toxicity for the patient [6]. These limitations of available systemic treatments for NSCLC emphasize the need for new approaches with improved efficacy and safety profiles [6].

Recently, increasing attention has been paid to the presence of specific and strongly over-expressed receptors, notably the epidermal growth factor receptor (EGFR), on the surface of cells of many cancer types including NSCLC [7]. The EGFR plays a key role in signalling pathways that regulate cell proliferation, angiogenesis and tumor metastasis [8]. EGFR signal transduction pathways are closely related to the occurrence and development of NSCLC, with about 80% of NSCLC tumors having high expression of the EGFR [9]. Cetuximab (Erbitux®, C225, Cet in the present paper), is a recombinant human/mouse chimeric monoclonal antibody that binds specifically to the extracellular domain of the human EGFR [10]. The drug was approved by the Food and Drug Administration in 2004 as a second-line treatment for advanced colorectal cancer [11,12]. It can competitively bind to extracellular ligand binding sites and thereby inhibit EGFR activation. As a result, tumor cell proliferation and angiogenesis are suppressed while apoptosis is stimulated. Cet is effective in suppressing proliferation and in enhancing apoptosis of malignant lung cells while it reduces lung cancer metastasis [13,14].

Both *in vitro* and in animal models of lung cancer, administering Cetuximab in combination with chemotherapy caused an additive effect on the apoptosis of lung cancer cells [15]. In clinical trials the impact of combination treatment of Cet with chemotherapeutic agents, was more important than with either treatment alone [16,17].

The combination of chemotherapy plus Cet was better than chemotherapy alone as the first-line treatment of advanced NSCLC in

* Corresponding authors.
E-mail addresses: male@nwu.edu.cn (L. Ma), chenmw0620@163.com (M. Chen).

https://doi.org/10.1016/j.jmmm.2019.01.021
Received 22 June 2018; Received in revised form 5 January 2019; Accepted 5 January 2019
Available online 07 January 2019
0304-8853/

improving overall survival [18,19]. At the same time it induced a higher rate of adverse events. Although these side effects were reported to be manageable, both the Food and Drug Administration and the European Medicines Agency decided to not accept the license for Cet in combination with chemotherapy for first-line therapy of advanced NSCLC because the limited improvement of overall survival did not outweigh the increased side effects and costs [19]. The treatment options for patients with locally advanced NSCLC remain thus poor today, with a rapidly declining survival rate from year 1 to year 2 of 88.9% to 51.9%, for stage III patients treated with combined Cet and chemotherapy [20].

Since the above mentioned decisions of the drug agencies not to accept the license for Cet in combination with chemotherapy for first-line therapy of advanced NSCLC further research in a tumor xenograft model demonstrated that conjugation of Cet with gold nanoparticles increased the cytotoxic effect on the strongly EGFR-expressing NSCLC A549 cell line in a dose-dependent manner [21]. Moreover, conjugation of Cet to dextran-coated superparamagnetic iron oxide nanoparticles led to a significant increase in apoptosis in EGFR-over-expressing cell lines [22]. More recently, Cet conjugated and Doxorubicin (Dox) loaded silica nanoparticles were shown to possess increased anti-cancer activity as compared with free Dox and Dox-loaded silica nanoparticles [23].

Dox is a broad-spectrum anticancer drug used for treatment of a number of solid tumors. In NSCLC cells, Dox treatment triggers activation of the unfolded protein response which subsequently promotes Dox-mediated apoptosis and caspase activation [24]. Clinical trials for advanced stages of NSCLC have revealed benefit for the treatment of this cancer type [25–27]. However, bone marrow toxicity and severe cardio-toxic effects of Dox limit the achievable therapeutic effect [28,29].

In earlier work, we have reported a new Dox drug magnetic delivery platform, Dox was loaded on dextran-coated Fe_3O_4 magnetic nanoparticles. In a rabbit model these drug-loaded nanoparticles, guided by an external magnetic field, showed a lower systemic toxicity [30] and led to an anti-tumor efficacy that was superior to that of free Dox [31]. In the present paper, we aimed to develop a convenient drug delivery system based on Fe_3O_4 magnetic nanoparticles with the potential to be active in locally advanced NSCLC. Dox and Cet conjugated dextran-coated Fe_3O_4 nanoparticles (Dox-NPs-Cet) were prepared and characterised. Then, they were incubated with A549 cells, a NSCLC cell line, which, as mentioned, over-expresses the EGFR [32,33] (Fig. 1), Finally, the internalization of Dox-NPs-Cet was evaluated and the cytotoxic inductive effects were studied. Our tests indicated that the Dox-NPs-Cet conjugate could be a promising candidate for antibody targeted Dox therapy of NSCLC. Further studies will be needed to reveal the cell death mechanism and whether the conjugates may have a superior activity than chemotherapy alone against minimal residual disease in animal models and in NSCLC patients after surgery.

2. Materials and methods

2.1. Materials

Cetuximab (Erbitux®, C225) was purchased from Merck Serono Co., Ltd., Beijing, China. Doxorubicin hydrochloride was supplied by Beijing HVsf United Chemical materials Co., Ltd., Beijing, China. The Cell Counting Kit-8 (CCK-8) a cellular proliferation and cytotoxicity assay was obtained from Dojindo, Japan. The Bradford Protein Assay Kit was obtained from Beijing Solarbio Science & Technology Co., Ltd., China. Cell culture medium (Modified RPMI-1640 Medium) was obtained from GE Healthcare Life Science Hyclone Laboratories, Logan, Utah, USA. Fetal Bovine Serum (FBS) was purchased from Beijing Solarbio Science & Technology Co., Ltd., China. Trypsin was obtained from Gibco Co., Ltd., USA. Additionally, Fe_3O_4 magnetic nanoparticles were synthesized by Xi'an GoldMag Nanobiotech Co., Ltd., China. Dextran-40 was purchased from Shanghai Huamao Pharmaceutical Co., Ltd. Iron salts were from Sigma-Aldrich (China) Co., Ltd. NaOH was purchased from Xi'an Fuli Chemical Reagents Co., Ltd., China. T-25 culture flasks, 96- and 6-well plates were obtained from Corning, USA. Protein Molecular Weight markers were purchased from Thermo Fisher Scientific, USA. Coomassie brilliant blue G250 was purchased from Beijing Solarbio Science & Technology Co., Ltd., China. The Magnetic Separator was obtained from Xi'an GoldMag Nanobiotech Co., Ltd., China. Water used in the experiments was de-ionized, and all organic solvents were of analytical reagent grade.

2.2. Preparation of dextran coated iron oxide nanoparticles.

Iron oxide magnetic nanoparticles were synthesized by Xi'an GoldMag Nanobiotech Co., Ltd., Xi'an, China. The preparation of dextran-coated nanoparticles was performed according to the method described earlier but with slight modifications [31]. Briefly, 5 g of dextran-40 were dissolved in 50 mL of a 0.5 M NaOH solution. After stirring for 10 min, the dextran-40 was completely dissolved. Subsequently, 1 g iron oxide magnetic particles, 50 mL NaOH and 2.686 g $Na_2HPO_4{\cdot}12H_2O$ were successively added to this solution. A black suspension was obtained. In order to remove an excess dextran and inorganic salts, dialysis was performed using membranes with a cut-off value of 10 KDa. This process was performed till the particles were brought to neutral pH. The dextran coated particles were used at room temperature for further characterization and for the experiments.

2.3. Loading of Doxorubicin on dextran-coated iron-oxide nanoparticles.

Dox was loaded on dextran-coated iron-oxide nanoparticles as follows: 15 mg of Dox dissolved in 15 mL of water was added into a flask containing 150 mg of the dextran-coated iron oxide particles under stirring (180 rpm). The reaction was continued at 37 °C for at least 24 h. Dox loaded nanoparticles (Dox-NPs) were separated by a magnetic separator. This instrument was applied for a period of three minutes and the loaded particles were stored at 4 °C for further use and characterization. The amount of Dox loaded was equal to the difference between the amount of free Dox before and after conjugation. The concentration of free Dox was monitored with UV–Vis spectrometry at 480 nm using a Shimadzu Corporation, UV-2550 Spectrophotometer.

2.4. Conjugation of Cetuximab on Dox-NPs

A quantity of 0.05 mL of a solution containing 100 µg Cet was slowly added into 1 mL of a solution containing 1 mg of Dox-NPs under continuous stirring for a period of 2 h at ambient temperature. The Cet and Dox loaded dextran coated iron oxide nanoparticles (Dox-NPs-Cet) were separated using a magnetic separator for a period of three minutes and stored at 4 °C for further use and characterisation. The amount of Cet loaded was equal to the difference between the amount of free Cet before and after conjugation. The concentration of free Cet was monitored by the Brandford method. The absorbance was read on an ELx-800 Universal Microplate Reader (BIOTEK Instrument, Vermont, USA) at 595 nm.

2.5. Investigation of the stability of the Dox-NPs-Cet.

In order to investigate the stability of the Cet conjugated on the Dox loaded dextran-coated iron-oxide nanoparticles in 0.01 M Tris-HCl (pH 7.4) at two different temperatures, 1 mg of the samples were cleaned using a magnetic separator and resuspended in 1 mL 0.01 M Tris-HCl (pH 7.4). The samples were then, kept at 4 °C in the refrigerator or at 37 °C in an incubator. Supernatants were taken after 0, 0.5, 1, 2, 4, 6 and 24 h. The magnetic separator was used to assure the absence of magnetic particles. Absorbance in the purified supernatant was measured at 595 nm (free Cet).

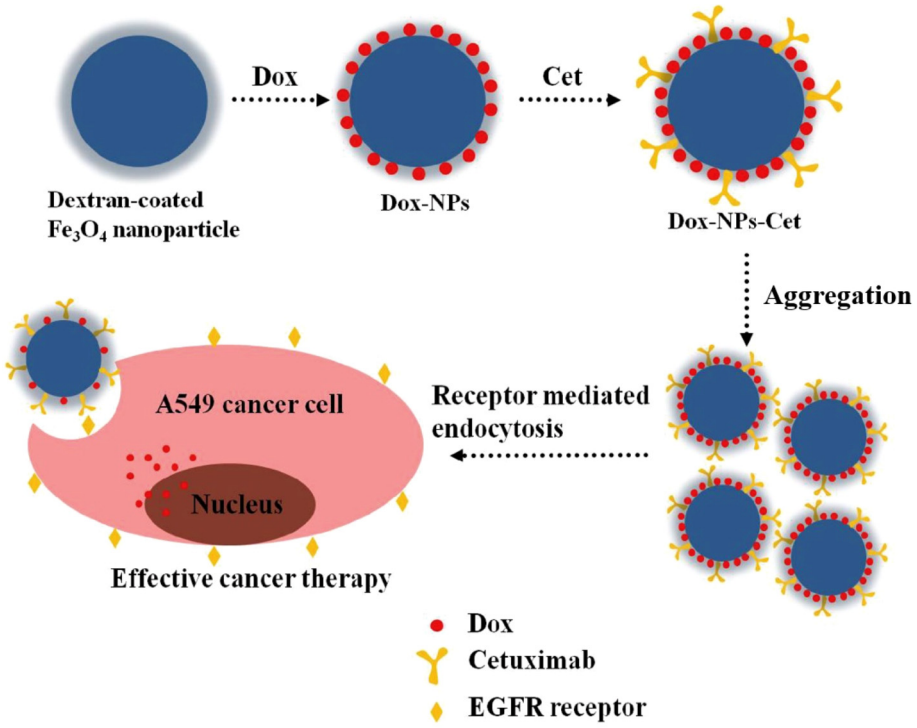

Fig. 1. Schematic illustration of the Dox-NPs-Cet therapy for non-small cell lung cancer (NSCLC).

2.6. Characterization of the nanocarriers

The particle sizes of the dextran-coated iron oxide particles and of the Cetuximab and Doxorubicin loaded dextran coated iron oxide nanoparticles were determined by using a Dynamic light scattering (DLS) instrument (Malvern Zetasizer Nano-ZS, Malvern Instrument, Worcestershire, UK). The morphology of the nanocarriers was studied by using a Transmission Electron Microscope (TEM) (Hitachi H-600, Hitachi Corporation, Tokyo, Japan). In order to characterise the composition of the nanocarriers, the presence of iron oxide bonds, the nature of the coating and its bonding on the surface Fourier transform infrared spectra (FTIR) were produced. These were recorded, using the KBr pellet technique, between 4000 and 400 cm^{-1} on a Nicolet 5700 FTIR spectrometer 60 (Thermo Nicolet 5700, Thermo Nicolet Corporation, Wisconsin, USA). Vibrating sample magnetometry (VSM) was used to measure the magnetic properties of the different nanocarriers with a magnetometer (LakeShore-655, Lake Shore Inc., USA), at room temperature.

2.7. Identification of the loaded-Cet using SDS-PAGE.

For SDS-PAGE, analysis, 30 µL of a Cet (2 mg/mL), Dox-NPs (1 mg/mL) and Dox-NPs-Cet (1 mg/mL) solution were mixed in an Eppendorf tube with 2 µL DTT (2 M) and 10 µL 4 × SDS-PAGE loading buffer (1 M Tris-HCl pH 6.8, 10% SDS, glycerol, bromophenol blue). Prior to the electrophoresis, the samples were heated in a boiling water bath for 10 min to assure protein denaturation. Then, 10 µL of the samples were loaded on a 12% SDS-PAGE gel. The same volume of the protein ladder mixture was used as a control. Electrophoresis was run at room temperature for 30 min at 80 V and subsequently at 120 V till the color indicator arrived at the bottom of the gel. Afterwards, the resulting gel was stained with Coomassie brilliant blue G250 in order to detect the protein bands.

2.8. Cell lines and cell culture

A549, adenocarcinomic human alveolar basal epithelial cells, originating from the Cell Bank of the Chinese Academy of Sciences (Shanghai, China), were kindly provided by Shaanxi Lifegen Co., Ltd Xi'an, China and cultured in T25 culture flasks in RPMI 1640 medium supplemented with 10% fetal bovine serum at 37 °C in a humidified 5% CO_2 atmosphere using a Thermo Scientific Forma Series II Water Jacket CO_2 incubator. The culture medium was renewed every 2–3 days and the cells were passaged at 1:2 every 2–3 days following trypsinization with 0.05% trypsin-EDTA.

2.9. In vitro cytotoxicity assays

Viability of A549 cells, cultured in the presence of dextran-coated particles, loaded or not loaded with Doxorubicin or/and Cetuximab, was determined using the CCK-8 assay. The test is based on the transformation by living cells of the highly water-soluble tetrazolium salt [2-(2-methoxy-4-nitrophenyl)-3-(4-nitrophenyl)-5-(2,4-disulfophenyl)-2H-tetrazolium, monosodium salt] into a water-soluble formazan dye. The quantity of the formazan dye produced is directly proportional to the number of living cells and has been shown to correlate with [3H]-thymidine incorporation. An A549 cell-suspension containing 5×10^3 cells/100 µL was seeded into wells of 96-well plates at 100 µL per well and incubated for 24 h in modified RPMI-1640. The medium was then removed and various concentrations of dextran-coated particles, loaded or not loaded with Doxorubicin or/and Cetuximab were added to the 96-well plates and incubated for 24 h or 48 h at 37 °C in a 5% CO_2 incubator. Various concentrations of Dox were obtained by dilution of Dox-NPs or Dox-NPs-Cet that we prepared at the beginning. After incubation, supernatants were removed, and all wells were washed twice with PBS buffer. Then, according to the manufacturer's operating instructions, 100 µL of 10% CCK-8 solution was added to each well after which the plate was placed in the incubator for 4 h. Subsequently the absorbance in each well was measured at 450 nm with the use of a microplate reader (Epoch Microplate Spectrophotometer, BioTek Instruments, Inc.). The cell viability rate (%) was calculated using the following formula: Cell viability rate (%) = [(As-Ab]]/[(Ac-Ab)] × 100%, where As is the absorbance of the experimental wells, Ac is the absorbance of the control wells and Ab is the absorbance of the

blank wells.

2.10. Internalization of the nanocarriers

To further confirm the intracellular uptake and localization of the nanocarriers, A549 cells were seeded at a density of 1×10^5 per well in 6-well plates (Corning, USA) and incubated for 24 h. Cells were treated with Dox-NPs-Cet in modified RPMI-1640 at 37 °C for 3 h. The cells were then trypsinized with 0.2 mL of a 0.25% trypsin solution per well (0.25%) after which they were washed twice with PBS and harvested. Cell fixation steps and placing on 400 mesh copper grids for TEM were performed according to standard protocols [35].

2.11. Statistical analysis

All values are expressed as the mean ± standard deviation (SD). GraphPad Prism 5.0 was used for the analysis of the experimental data. Statistical analysis of the data was performed using the T-test or the One-Way ANOVA-Ordinary test. A P value of less than 0.05 was considered statistically significant in all cases.

3. Results

3.1. Physicochemical properties of compound particles

The properties of dextran-coated nanoparticles and Dox-NPs-Cet were measured by TEM and Dynamic light scattering. TEM pictures show that Dox-NPs-Cet have better-dispersed than dextran-coated nanoparticles (Fig. 2A-a, b). On the basis of dynamic light scattering (DLS) measurements, the hydrodynamic diameter of Dox-NPs-Cet was determined as 144.5 nm with perfect size distribution, which is larger than that of the unmodified dextran-coated nanoparticles of 116.1 nm. This is because coating Cet on the surface of dextran-coated nanoparticles leads to a layer of adsorbed Cet protein which contributes to the hydrodynamic diameter. The diameter of Dox-NPs-Cet was in the appropriate range for a drug carrier [34].

To investigate whether the particles have been successfully coated, Dox-NPs-Cet were analyzed by FTIR. The FTIR spectra of dextran-coated nanoparticles, Dox-NPs and Dox-NPs-Cet are depicted in Fig. 2C. The FTIR spectrum for dextran-coated Fe_3O_4 particles shows that the characteristic absorption bands at 583 cm^{-1} belong to the Fe-O bonds, the absorption peaks at 3600–3200 cm^{-1} and 1150–1085 cm^{-1} are attributed to the O–H and C–O–C bonds (Fig. 2C-a). In addition, Fig. 2C-c shows the typical absorption peaks of Dox-NPs-Cet in the range of 1600–1700 cm^{-1} where the amide group absorbs [1]. The results indicate that dextran-coated Fe_3O_4 nanoparticles were successfully loaded with Dox and Cet. Furthermore, the amounts of Dox and Cet loaded on 1 mg dextran-coated Fe_3O_4 nanoparticles were measured. They were 41.5 ± 0.84 μg (Dox) and 36.24 ± 0.184 μg (Cet).

In further analyses, the magnetic properties of the nanoparticles were studied with VSM (Vibrating Sample Magnetometry) at room temperature. As shown in Fig. 2B, the magnetization of dextran loaded particles was 10.0 emu/g. After conjugation with Dox and Cet, it was 4.6 emu/g. This probably relates to the increase of the coating layer and the decrease of the mass percentage of iron oxide. Although the magnetization was reduced, the nanoparticles could still be successfully controlled using magnetic forces and they had a better magnetic responsiveness (Fig. 2E). When removed with a magnetic field, Dox-NPs-Cet nanoparticles remained well dispersed without a magnetic memory. This is very beneficial for the separation operation during co-conjugate preparation.

3.2. The result of SDS-PAGE and the stability of Dox-NPs-Cet

SDS-PAGE analysis was used to verify whether Cet was indeed loaded on the surface of the Dox-NPs. Fig. 3A shows the SDS gel confirming the presence of the Cet antibody on the Dox-NPs-Cet. Two bands are present in lane 2 where Cetuximab alone has been applied. In lane 4, where Dox-NPs-Cet have been applied, both the heavy chain and the light chain of the antibody can also be distinguished. The bands in lane 2 and lane 4 have the same molecular weights. The results of SDS-PAGE indicate a successful coating of Dox-NPs with Cet.

The stability of Dox-NPs-Cet was determined by evaluating the released amount of Cet in its storage buffer, 0.01 M Tris-HCl (pH7.4), over a period of 24 h. Samples were respectively incubated at 4 °C or at 37 °C for 0.5 h, 1 h, 2 h, 4 h, 6 h and 24 h. Subsequently the particles were separated by the magnetic separator. Supernatants were collected and measured. As shown in Fig. 3B, whether at 4 °C or at 37 °C, the release of Cet always started from the 4th hour. Between 4 and 24 h, only about 20% of Cet was gradually released from the particles. This suggests that Dox-NPs-Cet are relatively stable in the storage buffer.

3.3. Internalization of the nanocarriers

We use TEM to observe whether the particles entered the cells and to study the sub-cellular distribution of these particles. As shown in

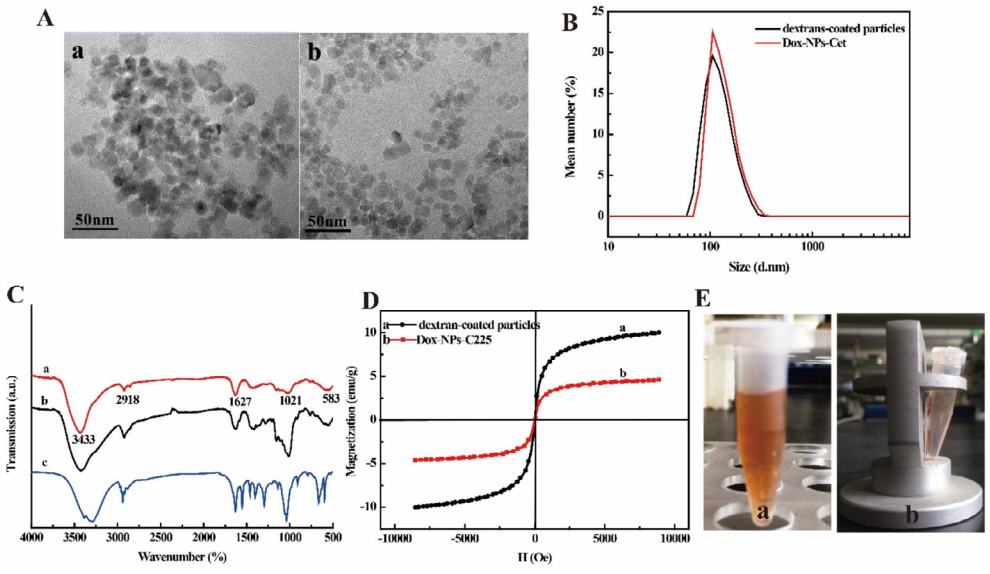

Fig. 2. The characterization of Dox-NPs-Cet. A) Representative transmission electron microscope (TEM) images of (a) dextran-coated nanoparticles (b) Dox-NPs-Cet. B) The hydrodynamic size of Dox-NPs-Cet and that of dextran-coated nanoparticles measured by dynamic light scattering. C) The FTIR spectra of (a) dextran-coated nanoparticles (b) Dox-NPs (c) Dox-NPs-Cet. D) The magnetization curves of dextran-coated nanoparticles and Dox-NPs-Cet. E) The Dox-NPs-Cet suspension without (left) and with (right) a magnet in its vicinity.

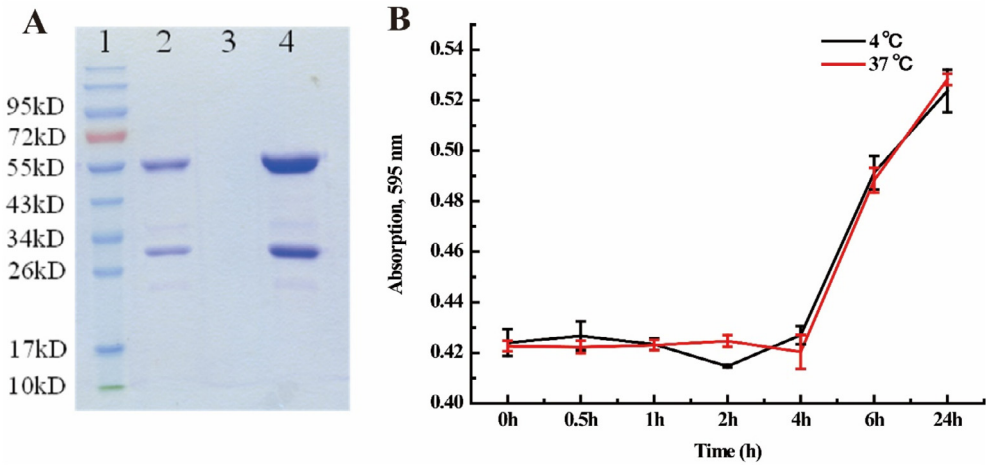

Fig. 3. A) The SDS-PAGE images of the gel after Coomassie blue staining. Lane 1: molecular markers; Lane 2: Cetuximab only; Lane 3: Dox-NPs (negative control); Lane 4: Dox-NPs-Cet. B) The stability of Dox-NPs-Cet in 0.01M Tris-HCl (pH7.4) at two different temperatures.

Fig. 4, Dox-NPs-Cet were internalized into A549 cells. The nanoparticles can be clearly observed both at the cell membrane and in vesicles in the cells. Arrows are used to show typical examples of the localization of Dox-NPs-Cet targeting nanocarriers within the cells. Fig. 4A represents control cells untreated with nanoparticles. As shown in Fig. 4B, aggregated particles were found on the surface of the cell membranes. This might be due to the specific targeting of the EGFR with the monoclonal antibody Cet. However we only observed Dox-NPs-Cet on parts of the cell membranes. In Fig. 4C, proof of cellular uptake of the Dox-NPs-Cet is visible on the TEM image. The nanoparticles are present in cellular vesicles. In Fig. 4D, larger aggregates of particles are found in the cells. These results indicate that the small sized nanoparticles were efficient in targeting the cells and were easily internalized in endosomes.

3.4. In vitro cytotoxicity of dextran-coated Fe_3O_4 nanoparticles, Dox-NPs and Dox-NPs-Cet

To evaluate the cytotoxicity for A549 tumor cells of Dox-NPs-Cet as compared to that of dextran-coated Fe_3O_4 nanoparticles, Cet and Dox-NPs, A549 cells were incubated with these compounds for 24 h and 48 h in the following concentration ranges: dextran-coated Fe_3O_4 nanoparticles (25–1000 μg/mL), Cet solution (10–500 μg/mL), Dox-NPs (Dox: 0.1–2 μg/mL) and Dox-NPs-Cet (Dox: 0.1–2 μg/mL).

As shown in Fig. 5, when treated with dextran-coated Fe_3O_4 nanoparticles in the concentration range of 25–1000 μg/mL, viability of the A549 cells exceeded 85% at all concentrations (Fig. 5A). This demonstrates that dextran-coated Fe_3O_4 nanoparticles have a good biocompatibility with A549 cells. When cells were co-cultured with Cet alone (Fig. 5B), cell viability was affected slightly and there was no statistically significant difference between the various concentrations

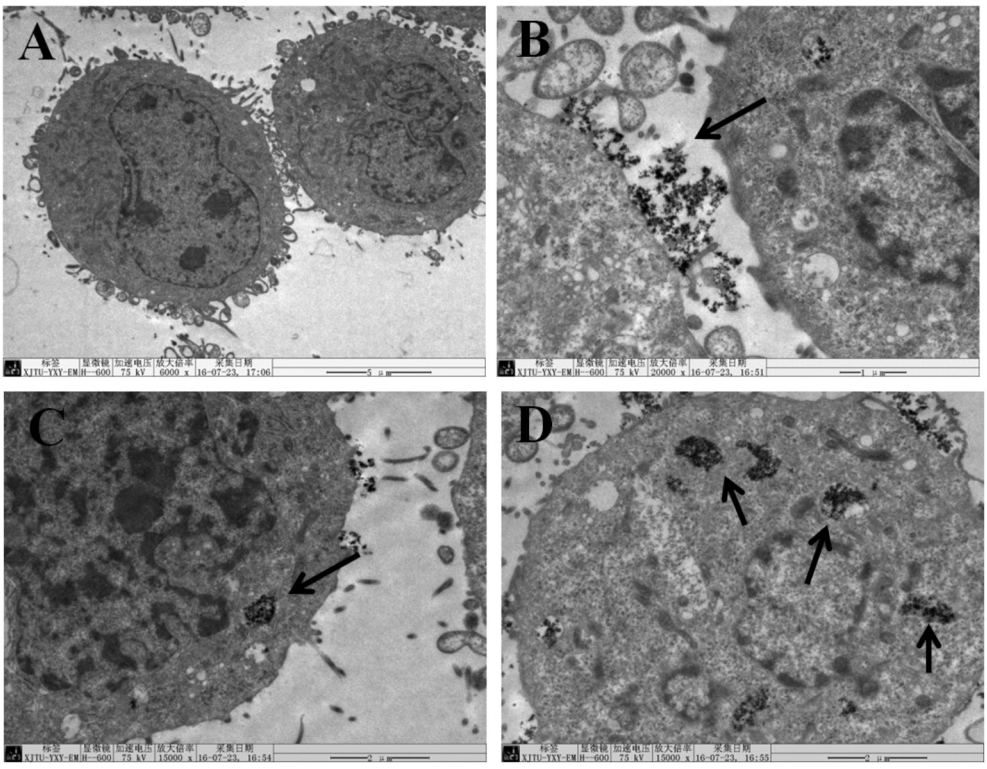

Fig. 4. Representative TEM images of A549 control cells and A549 cells treated with Dox-NPs-Cet in modified RPMI-1640 at 37 °C for 3 h. Nanoparticles were located at the cell membrane and in intracellular vesicles in which they form large aggregates. Arrows are used to show typical examples of the localization of Dox-NPs-Cet targeting nanocarriers within the cells. A) Control cells, not treated. B) Nanocarriers concentrate near some sites of the plasma membrane. C) A typical example of nanocarriers concentrated in an intracellular vesicle (arrow). Some particles can also be seen in the vicinity of the plasma membrane. D) Typical examples of large aggregates of nanocarriers concentrated in endosomes (arrows).

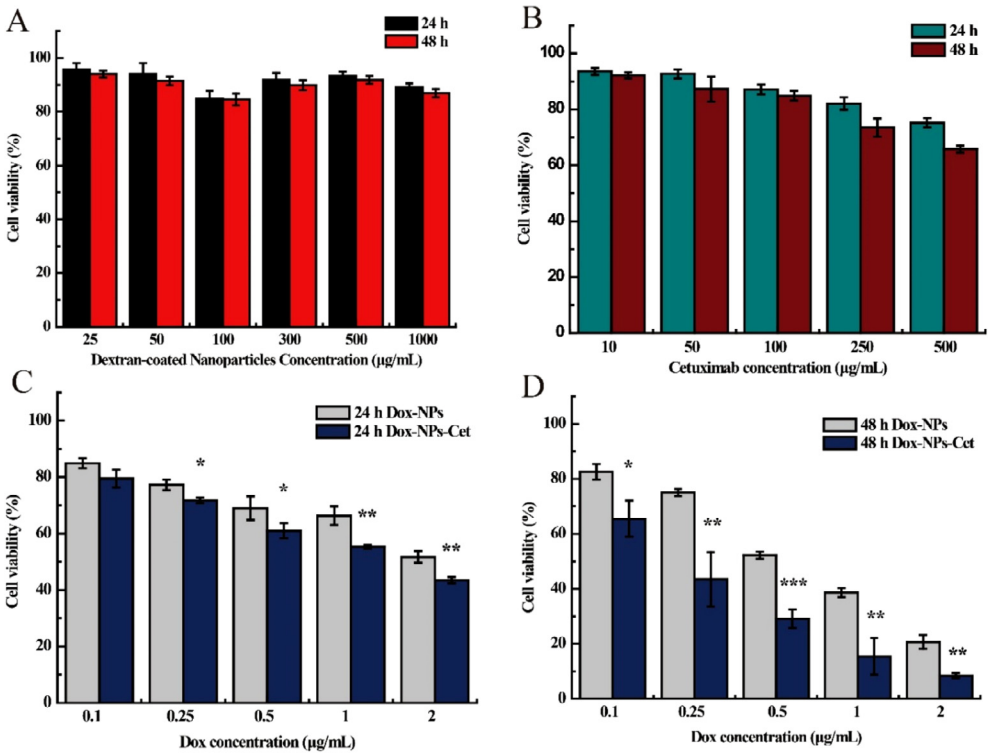

Fig. 5. *In vitro* cell viability of A 549 cells co-incubated with dextran-coated Fe_3O_4 nanoparticles (NPs), Cet, Dox-NPs and Dox-NPs-Cet as measured by the CCK-8 assay. Cytotoxic effect of A) dextran-coated Fe_3O_4 nanoparticles (NPs), B) Cet alone, C) & D) Dox-NPs and Dox-NPs-Cet incubated with A549 cells for 24 h and 48 h respectively at different concentrations equivalent to the Dox concentrations indicated. Values represent the means ± SD. (***P < 0.001; **P < 0.01; * P < 0.05).

and culture times. However, when incubated with Dox-NPs or with Dox-NPs-Cet a significant reduction of the viability of the A549 cells followed and this was already the case after 24 h. Stronger inhibition could be observed after 48 h. The IC50 value of Dox-NPs-Cet at 48 h (0.22 μg/mL) is much lower than that of Dox-NPs (0.68 μg/mL), indicating that conjugating Dox-NPs with Cet significantly increases the cytotoxicity of Dox-NPs (Fig. 5C, D).

4. Discussion

In this report, we synthesized co-conjugates of Cetuximab and Doxorubicin loaded on dextran-coated Fe_3O_4 magnetic nanoparticles (Dox-NPs-Cet) as novel targeted nanocarriers for potential use in non-small cell lung cancer treatment. The chemical composition and physicochemical properties of the co-conjugates were analysed by FTIR, VSM, DLS, and SDS-PAGE. Coating of dextran-coated Fe_3O_4 magnetic nanoparticles with Dox and Cet was shown to be successful. The co-conjugated particles were shown by TEM to have an appropriate hydrodynamic size of 144.5 nm, in the range of 100–200 nm, which allowed them to easily enter into the cell [34]. Large aggregates of Dox-NPs-Cet were found in the cells. Dox-NPs-Cet show cytotoxicity effects on A549 cell, a NSCLC cell line expressing the wild-type EGFR. The cytotoxicity test demonstrated that Cetuximab loaded Dox-NPs significantly reduced the cell viability in a dose-dependent manner. While the dextran-coated Fe_3O_4 magnetic nanoparticles were biocompatible with A549 cells and showed no concentration dependent cytotoxic effects.

As a delivery system in relation to Doxorubicin and Cetuximab, the dextran-coated Fe_3O_4 magnetic nanoparticles provided a large solid surface for drug loading. This could improve the drugs pharmacokinetics and biological distribution [36]. Furthermore, magnetic nanoparticles greatly facilitated the co-conjugate preparation process which is an important factor for a good anticancer nanomedicine [37].

As mentioned above, the majority of patients with NSCLC present with already locally advanced or metastasised disease at the moment of diagnosis. Local treatments including surgery and radiotherapy and their combinations, very effective for local disease, are therefore insufficiently effective for the majority of patients. In recent years significant research efforts have been made in mouse models to use magnetic nanoparticles for improving loco-regional cancer treatment. Some studies have focused on targeting drug loaded particles to the vicinity of the tumor with the use of an external magnetic field [30] while others target the particles to the tumor tissue using for example a monoclonal antibody like Cet and subsequently apply an alternating magnetic field to induce hyperthermia in the tumor area [38]. However, the traditional loco-regional treatments cannot be used to treat micro-metastases or circulating cancer cells that cannot be detected by existing imaging techniques. These micrometastases and circulating tumor cells lead to a high rate of cancer treatment failure and the effect of existing systemic treatments on the cure rate of NSCLC patients is, so far, regrettably poor.

It is therefore, in the present work, not our only goal to develop nanocarriers for the improvement of loco-regional treatments. On the contrary we developed a versatile platform with the potential to also treat minimal residual disease, after local treatments have been applied. We demonstrated that our carriers can be used for targeted drug delivery and in view of their superparamagnetic nature and their ability to be magnetically manipulated they can also be used for guidance by a magnetic field and for hyperthermia. In this respect our co-conjugates of Cet and Dox loaded on dextran-coated Fe_3O_4 magnetic nanoparticles offer a significant advantage as compared with Cet conjugated and dox loaded silica nanoparticles [23].

The capacity to magnetically manipulate the co-conjugates is also highly important for testing their capacity to prohibit or delay growth of micro-metastases in animal models. After injection of cancer cells in the tail vein of laboratory animals, micro-metastases will develop first in the lungs [39]. Treatment with the Cet and Dox loaded dextran-coated Fe_3O_4 magnetic nanoparticles is expected to delay this development. Magnetic manipulation of the co-conjugates to another part of the body of the animal during administration, forms an important control experiment needed for demonstrating that the therapeutic benefit obtained is related to the local action of the co-conjugate on the micro-metastases.

5. Conclusion

Our results clearly demonstrate that dextran coated Fe_3O_4 nanoparticles can be efficiently conjugated with both a cytostatic drug and a targeting monoclonal antibody. The nanocarriers are taken up by the cells and the bound chemotherapeutic is released after which it reduces the viability of the tumor cells. Our nanocarriers form versatile tools that can be used for improving loco regional control by application of a magnetic field for increasing the drug concentration in the tumor vicinity or of an alternating magnetic field for inducing hyperthermia. They will, more importantly, also facilitate research aiming at evaluating their capacity to influence cancer progression at the level of micrometastases. While Cetuximab forms an efficient monoclonal antibody for targeting EGFR expressing tumors, future research may lead to even more efficient antibodies, for example with a higher binding affinity for the EGFR [40]. Such monoclonal antibodies may in the future be used for more efficiently targeting potent drugs like Doxorubicin or Cisplatin to NSCLC cells in order to further increase the specific toxicity to the tumor cells thereby limiting side effects in other tissues.

Acknowledgements

This work was supported by the Science and Technology Research and Development Program of the Shaanxi Province of the P.R. China with grant numbers 2014K13-11 and 2017ZDXM-SF-056.

References

[1] W. Chen, R. Zheng, P.D. Baade, S. Zhang, H. Zeng, F. Bray, A. Jemal, X.Q. Yu, J. He, Cancer statistics in China, 2015, CA Cancer J Clin 66 (2) (2016) 115–132.
[2] L.A. Torre, F. Bray, R.L. Siegel, J. Ferlay, J. Lortet-Tieulent, A. Jemal, Global cancer statistics, 2012, CA Cancer J Clin 65 (2) (2015) 87–108.
[3] W. Chen, S. Zhang, X. Zou, Estimation and projection of lung cancer incidence and mortality in China, Zhongguo Fei Ai Za Zhi 13 (5) (2010) 488–493.
[4] E. Harper, W. Dang, R.G. Lapidus, R.I. Garver Jr., Enhanced efficacy of a novel controlled release paclitaxel formulation (PACLIMER delivery system) for local-regional therapy of lung cancer tumor nodules in mice, Clin Cancer Res 5 (12) (1999) 4242–4248.
[5] A. Auperin, C. Le Pechoux, E. Rolland, W.J. Curran, K. Furuse, et al., Meta-analysis of concomitant versus sequential radiochemotherapy in locally advanced non-small-cell lung cancer, J Clin Oncol 28 (13) (2010) 2181–2190.
[6] H.A. Burris 3rd, Shortcomings of current therapies for non-small-cell lung cancer: unmet medical needs, Oncogene 28 (Suppl 1) (2009) S4–S13.
[7] E. Castanon, P. Martin, C. Rolfo, J.P. Fusco, L. Ceniceros, J. Legaspi, M. Santisteban, I. Gil-Bazo, Epidermal Growth Factor Receptor targeting in non-small cell lung cancer: revisiting different strategies against the same target, Curr Drug Targets 15 (14) (2014) 1273–1283.
[8] J. Baselga, Why the epidermal growth factor receptor? The rationale for cancer therapy, Oncologist 7 (Suppl 4) (2002) 2–8.
[9] R. Danesi, G. Pasqualetti, E. Giovannetti, F. Crea, G. Altavilla, M. Del Tacca, R. Rosell, Pharmacogenomics in non-small-cell lung cancer chemotherapy, Adv Drug Deliv Rev 61 (5) (2009) 408–417.
[10] G. Privitera, T. Luca, N. Musso, C. Vancheri, N. Crimi, V. Barresi, D. Condorelli, S. Castorina, In vitro antiproliferative effect of trastuzumab (Herceptin((R))) combined with cetuximab (Erbitux((R))) in a model of human non-small cell lung cancer expressing EGFR and HER2, Clin Exp Med 16 (2) (2016) 161–168.
[11] R. Roskoski Jr., The ErbB/HER family of protein-tyrosine kinases and cancer, Pharmacol Res 79 (2014) 34–74.
[12] R.J. Cersosimo, Management of advanced colorectal cancer, Part 1, Am J Health Syst Pharm 70 (5) (2013) 395–406.
[13] M.D. Marmor, K.B. Skaria, Y. Yarden, Signal transduction and oncogenesis by ErbB/HER receptors, Int J Radiat Oncol Biol Phys 58 (3) (2004) 903–913.
[14] D. Raben, B. Helfrich, D.C. Chan, F. Ciardiello, L. Zhao, et al., The effects of cetuximab alone and in combination with radiation and/or chemotherapy in lung cancer, Clin Cancer Res 11 (2 Pt 1) (2005) 795–805.
[15] N. Hanna, R. Lilenbaum, R. Ansari, T. Lynch, R. Govindan, P.A. Janne, P. Bonomi, Phase II trial of cetuximab in patients with previously treated non-small-cell lung cancer, J Clin Oncol 24 (33) (2006) 5253–5258.
[16] F. Robert, G. Blumenschein, R.S. Herbst, F.V. Fossella, J. Tseng, M.N. Saleh, M. Needle, Phase I/IIa study of cetuximab with gemcitabine plus carboplatin in patients with chemotherapy-naive advanced non-small-cell lung cancer, J Clin Oncol 23 (36) (2005) 9089–9096.
[17] C.D. Thienelt, P.A. Bunn Jr., N. Hanna, A. Rosenberg, M.N. Needle, M.E. Long, D.L. Gustafson, K. Kelly, Multicenter phase I/II study of cetuximab with paclitaxel and carboplatin in untreated patients with stage IV non-small-cell lung cancer, J Clin Oncol 23 (34) (2005) 8786–8793.
[18] R. Rosell, G. Robinet, A. Szczesna, R. Ramlau, M. Constenla, et al., Randomized phase II study of cetuximab plus cisplatin/vinorelbine compared with cisplatin/vinorelbine alone as first-line therapy in EGFR-expressing advanced non-small-cell lung cancer, Ann Oncol 19 (2) (2008) 362–369.
[19] Z.Y. Yang, L. Liu, C. Mao, X.Y. Wu, Y.F. Huang, X.F. Hu, J.L. Tang, Chemotherapy with cetuximab versus chemotherapy alone for chemotherapy-naive advanced non-small cell lung cancer, Cochrane Database Syst Rev 11 (2014) CD009948.
[20] D. Liu, X. Zheng, J. Chen, G. Liu, Y. Xu, et al., Induction chemotherapy with cetuximab, vinorelbine-cisplatin followed by thoracic radiotherapy and concurrent cetuximab, vinorelbine-cisplatin in patients with unresectable stage III non-small cell lung cancer, Lung Cancer 89 (3) (2015) 249–254.
[21] Y. Qian, M. Qiu, Q. Wu, Y. Tian, Y. Zhang, N. Gu, S. Li, L. Xu, R. Yin, Enhanced cytotoxic activity of cetuximab in EGFR-positive lung cancer by conjugating with gold nanoparticles, Sci Rep 4 (2014) 7490.
[22] S.H. Tseng, M.Y. Chou, I.M. Chu, Cetuximab-conjugated iron oxide nanoparticles for cancer imaging and therapy, Int J Nanomed 10 (2015) 3663–3685.
[23] J.K. Wang, Y.Y. Zhou, S.J. Guo, Y.Y. Wang, C.J. Nie, et al., Cetuximab conjugated and doxorubicin loaded silica nanoparticles for tumor-targeting and tumor microenvironment responsive binary drug delivery of liver cancer therapy, Mater Sci Eng C Mater Biol Appl 76 (2017) 944–950.
[24] X. Zhao, Y. Yang, F. Yao, B. Xiao, Y. Cheng, et al., Unfolded protein response promotes doxorubicin-induced nonsmall cell lung cancer cells apoptosis via the mTOR pathway inhibition, Cancer Biother Radiopharm 31 (10) (2016) 347–351.
[25] M.I. Koukourakis, K. Romanidis, M. Froudarakis, G. Kyrgias, G.V. Koukourakis, G. Retalis, N. Bahlitzanakis, Concurrent administration of Docetaxel and Stealth liposomal doxorubicin with radiotherapy in non-small cell lung cancer: excellent tolerance using subcutaneous amifostine for cytoprotection, Br J Cancer 87 (4) (2002) 385–392.
[26] G. Numico, F. Castiglione, C. Granetto, O. Garrone, G. Mariani, et al., Single-agent pegylated liposomal doxorubicin (Caelix) in chemotherapy pretreated non-small cell lung cancer patients: a pilot trial, Lung Cancer 35 (1) (2002) 59–64.
[27] R.A. Joss, P. Alberto, J.P. Obrecht, L. Barrelet, E.E. Holdener, P. Siegenthaler, A. Goldhirsch, B. Mermillod, F. Cavalli, Combination chemotherapy for non-small cell lung cancer with doxorubicin and mitomycin or cisplatin and etoposide, Cancer Treat Rep 68 (9) (1984) 1079–1084.
[28] S. Kumar, R. Marfatia, S. Tannenbaum, C. Yang, E. Avelar, Doxorubicin-induced cardiomyopathy 17 years after chemotherapy, Tex Heart Inst J 39 (3) (2012) 424–427.
[29] T. Loncar-Turukalo, M. Vasic, T. Tasic, G. Mijatovic, S. Glumac, D. Bajic, N. Japunzic-Zigon, Heart rate dynamics in doxorubicin-induced cardiomyopathy, Physiol Meas 36 (4) (2015) 727–739.
[30] X. Chao, Z. Zhang, L. Guo, J. Zhu, M. Peng, A.J. Vermorken, W.J. Van de Ven, C. Chen, Y. Cui, A novel magnetic nanoparticle drug carrier for enhanced cancer chemotherapy, PLoS One 7 (10) (2012) e40388.
[31] M. Peng, H. Li, Z. Luo, J. Kong, Y. Wan, et al., Dextran-coated superparamagnetic nanoparticles as potential cancer drug carriers in vivo, Nanoscale 7 (25) (2015) 11155–11162.
[32] I.Y. Kim, Y.S. Kang, D.S. Lee, H.J. Park, E.K. Choi, Y.K. Oh, H.J. Son, J.S. Kim, Antitumor activity of EGFR targeted pH-sensitive immunoliposomes encapsulating gemcitabine in A549 xenograft nude mice, J Control Release 140 (1) (2009) 55–60.
[33] J. Li, Y. Li, Z.Q. Feng, X.G. Chen, Anti-tumor activity of a novel EGFR tyrosine kinase inhibitor against human NSCLC in vitro and in vivo, Cancer Lett 279 (2) (2009) 213–220.
[34] U. Jeong, T. Herricks, E. Shahar, Y. Xia, Amorphous Se: a new platform for synthesizing superparamagnetic colloids with controllable surfaces, J Am Chem Soc. 127 (4) (2005) 1098–1099.
[35] B.D. Chithrani, A.A. Ghazani, W.C. Chan, Determining the size and shape dependence of gold nanoparticle uptake into mammalian cells, Nano Lett 6 (4) (2006) 662–668.
[36] F. Alexis, E. Pridgen, L.K. Molnar, O.C. Farokhzad, Factors affecting the clearance and biodistribution of polymeric nanoparticles, Mol Pharm 5 (4) (2008) 505–515.
[37] S.D. Li, L. Huang, Pharmacokinetics and biodistribution of nanoparticles, Mol Pharm 5 (4) (2008) 496–504.
[38] T. Sadhukha, T.S. Wiedmann, J. Panyam, Inhalable magnetic nanoparticles for targeted hyperthermia in lung cancer therapy, Biomaterials. 34 (21) (2013) 5163–5171.
[39] C. Khanna, K. Hunter, Modeling metastasis in vivo, Carcinogenesis 26 (3) (2005) 513–523.
[40] H.N. Kang, S.H. Kim, M.R. Yun, H.R. Kim, S.M. Lim, et al., ER2, a novel human anti-EGFR monoclonal antibody inhibit tumor activity in non-small cell lung cancer models, Lung Cancer 95 (2016) 57–64.